Supplementary Information

A one-step fabrication method for CNT–QD hybrid 3D architectures with engineered optoelectronic properties

Jaemin Kim[a,†], Hyeongjip Kim[b,†], Ye-Won Lee[c,†], Seong-Jae Eom[a], Hyeon-Seok Seo[b], Sun-Hwa Gu[b], Sunghyun Kwak[c], Jae-Hyeon Ko[c], Won-Geun Kim[b,d,], Jong-Min Lee [a,c,*]*

[a]School of Semiconductor·Display Technology, Hallym University, Chuncheon 24252, Republic of Korea

[b]2Department of Optical Engineering, Kumoh National Institute of Technology, Gumi 39177, Republic of Korea

[c]School of Nano Convergence Technology & Nano Convergence Technology Center, Hallym University, Chuncheon 24252, Republic of Korea

[d]Department of Physcis, Kumoh National Institute of Technology, Gumi 39177, Republic of Korea

*Corresponding authors. E-mail: wgkim@kumoh.ac.kr (W.-G. Kim) & jmlee@hallym.ac.kr (J. Lee)

†These authors contributed equally to this work.

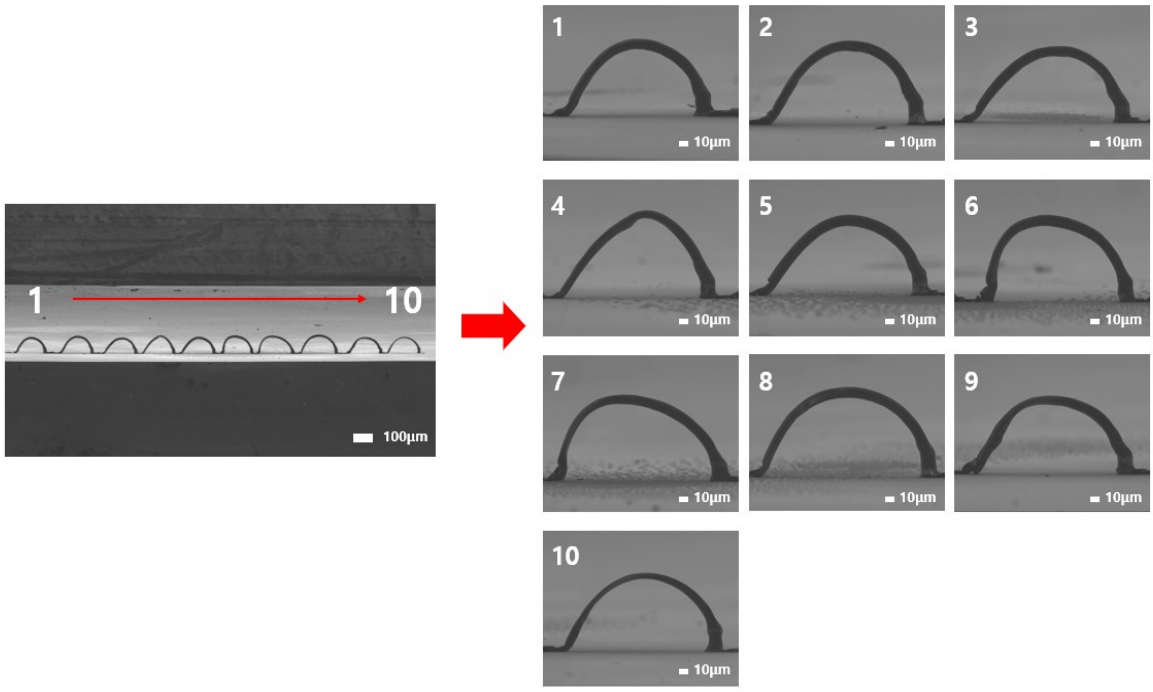

Supplementary Figure S1. Reproducibility and quantitative yield of micropipette-based printed CNT architectures.

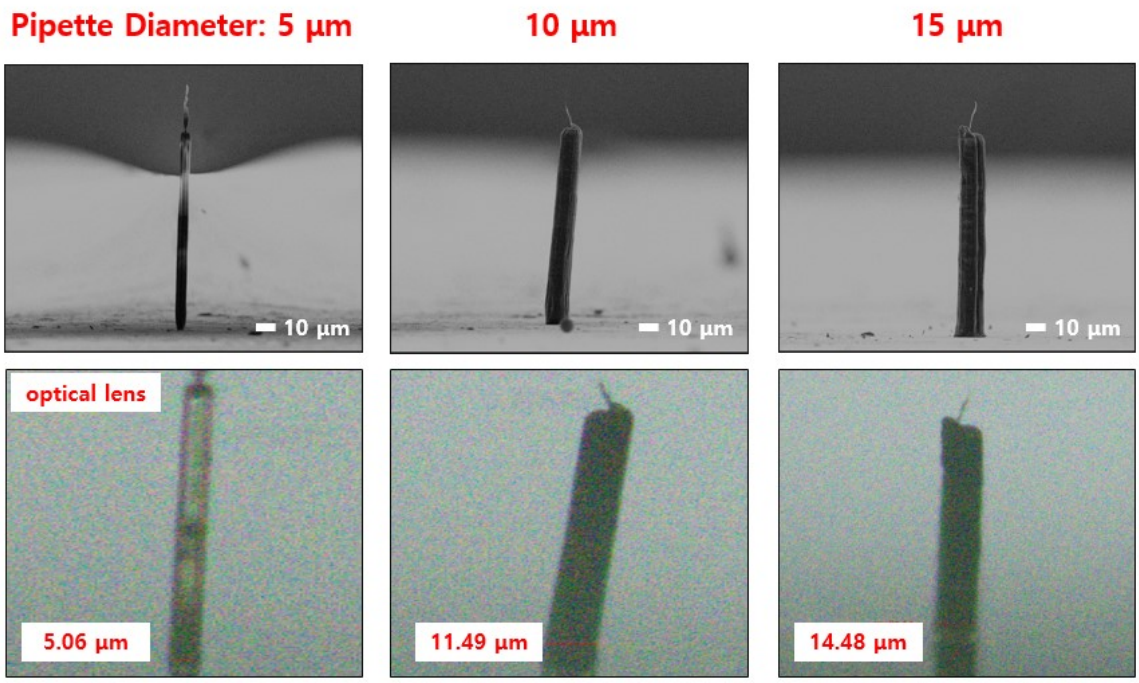

Supplementary Figure S2. Diameter-controlled fabrication of CNT–QD pillar structures using glass micropipettes with different tip aperture sizes.

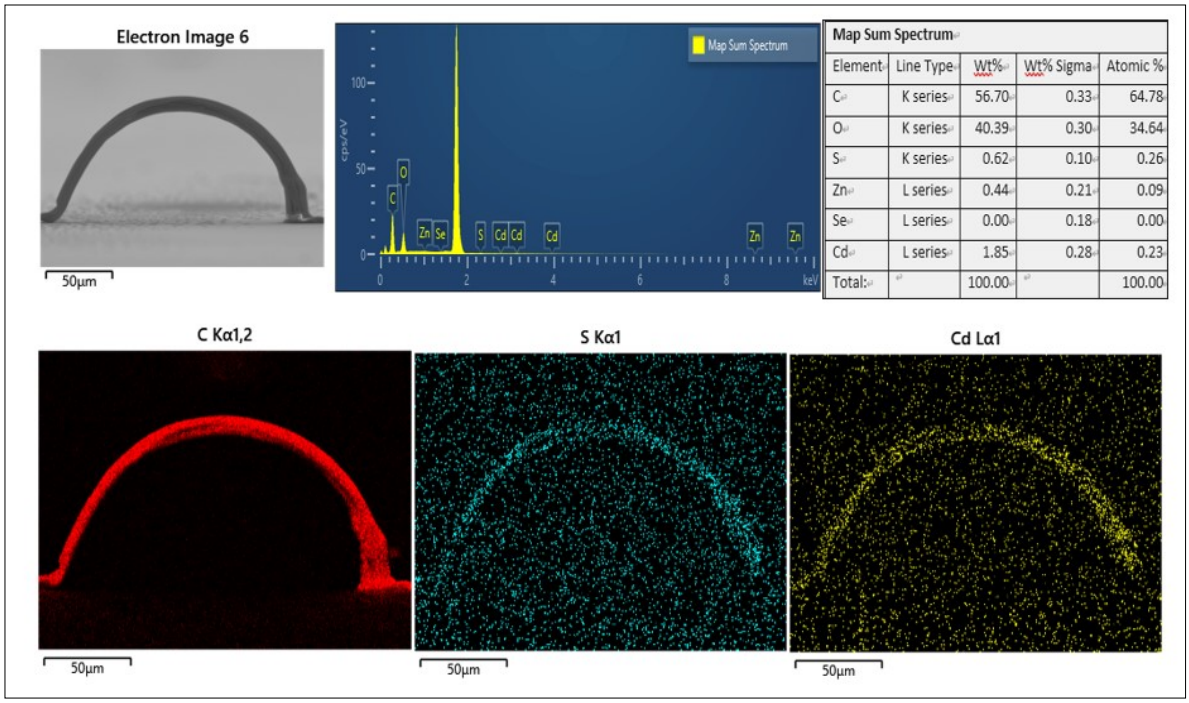

Map Sum Spectrum				
Element	Line Type	Wt%	Wt% Sigma	Atomic %
C	K series	56.70	0.33	64.78
O	K series	40.39	0.30	34.64
S	K series	0.62	0.10	0.26
Zn	L series	0.44	0.21	0.09
Se	L series	0.00	0.18	0.00
Cd	L series	1.85	0.28	0.23
Total:		100.00		100.00

Supplementary Figure S3. SEM–EDX elemental mapping of CNT–QD hybrid architectures.

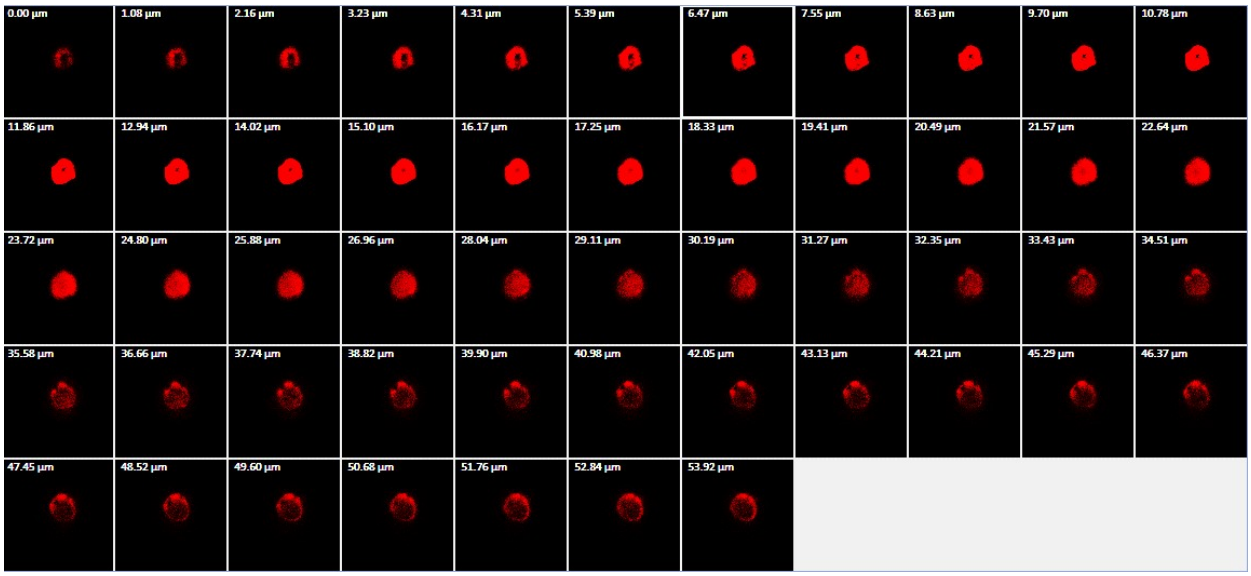

Supplementary Figure S4. PL cross-sections measured at ~1 µm intervals using a confocal PL measurement system.

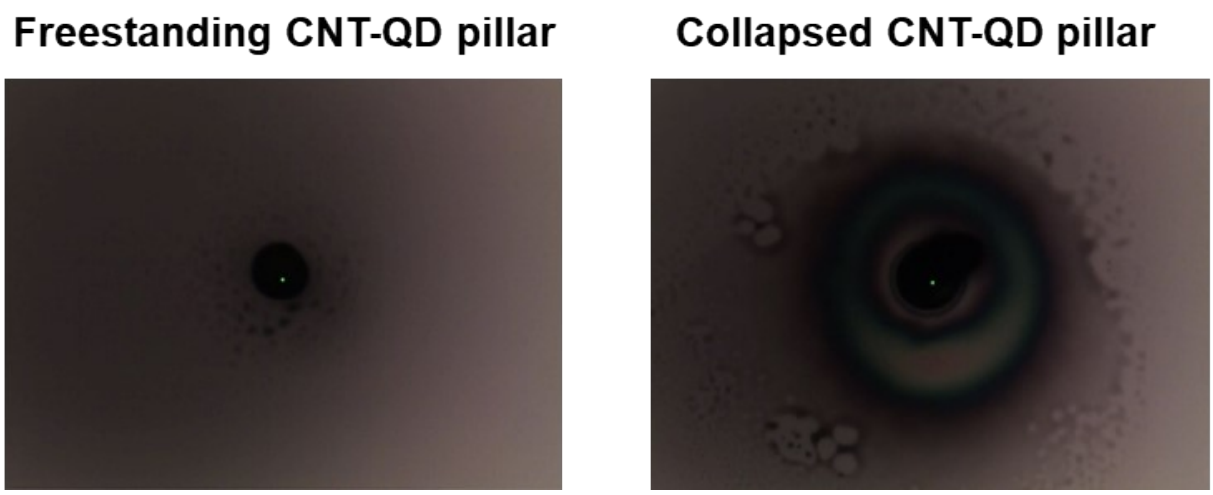

Supplementary Figure S5. Optical microscope images of freestanding CNT–QD pillars and collapsed CNT–QD pillars caused by excessive laser power.

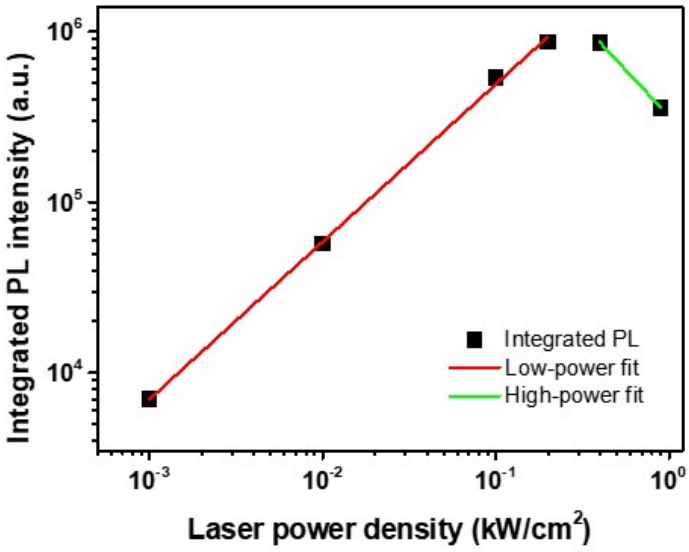

Supplementary Figure S6. Integrated PL intensity versus laser power density with power-law fits.

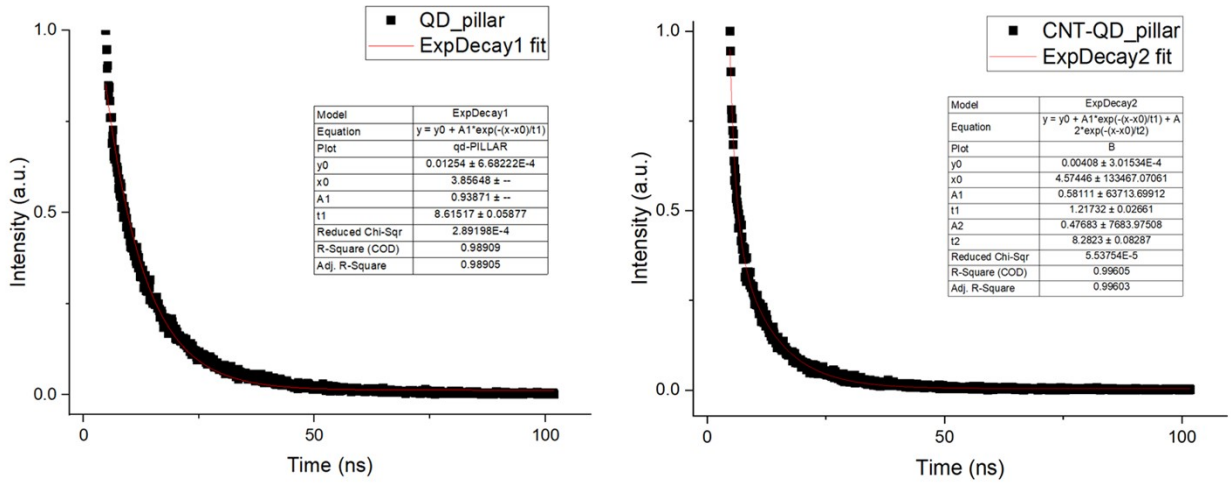

Supplementary Figure S7. Fitting results of time-resolved photoluminescence decay curves.